ENGINEERING TRANSACTIONS • *Engng. Trans.* • **61**, 1, 33–46, 2013
Polish Academy of Sciences • Institute of Fundamental Technological Research (IPPT PAN)
National Engineering School of Metz (ENIM)

Rubber Structure under Dynamic Loading – Computational Studies

Paweł BARANOWSKI, Roman GIELETA, Jerzy MAŁACHOWSKI, Łukasz MAZURKIEWICZ

Military University of Technology
Department of Mechanics and Applied Computer Science
Gen. S. Kaliskiego 2, 00-908 Warszawa, Poland
e-mail: pbaranowski@wat.edu.pl

This study focuses on the rubber structure behaviour assessment under dynamic loading using numerical methods. Dynamic simulations of the TNT explosion under the tire-suspension system were performed using the explicit LS-Dyna code using Arbitrary Lagrangian-Eulerian formulation with Jones Wilkins Lee (JWL) equation defining the explosive material. During analyses two different constitutive materials were used: Mooney-Rivlin without rate-dependency and Ogden rubberlike material (MAT 181 Simplified Rubber) which includes strain rate effects. Consequently, tire rubber material behaviour was investigated and compared for two simulated cases.

Key words: rubber, constitutive models, strain rate, dynamic loading, suspension system, tire.

1. Introduction

Due to its mechanical characteristics, including ability to reversible deformation under the loading of mechanical forces, rubber is very popular in various forms in many industries. One of these branches is the automotive industry, where materials and rubber-based composites are often used to produce tires with high strength and durability. Moreover, elastomeric structures because of their low modulus and high damping characteristics are used to absorb energy in dynamic loadings (impulse or impacts) as isolations bearings, shocks absorbers, etc. All above shows that an accurate assessment of their mechanical properties in various operational conditions have much importance in engineering applications. After material development there is a need to conduct experiments to determine the material properties and to validate a specific model of rubber.

Therefore, the dynamic behaviour of the elastomeric material at high and low strain rates have to be examined.

Mechanical properties of rubber in static experimental tests were effectively determined and understood [1, 2] and the behaviour under high-strain rates loading recently becomes more thoroughly investigated with both compression and tension characteristics taking into consideration. Based on literature review it can be noticed that majority of authors determined compression behaviour of elastomers using modified versions of Split Hopkinson Pressure Bar device [3–6] or using finite element method simulating various types of dynamic loading [7–9].

Several authors published results of the dynamic tensile tests, which were performed on the high speed extension device based on a Charpy impact tester [3, 10, 11], using the freely expanding ring technique [12, 13] or using the catapult apparatus [3]. Generally, rubber-like materials behaviour was assessed in strain rates between 200 s^{-1} (catapult apparatus) through 435 s^{-1} (Charpy impact tester) up to 13800 s^{-1} (expanding ring). Based on above it can be concluded that mechanical behaviour of major elastomeric structures mainly depends on large strains, high strain rate (above 10 s^{-1}) and nonlinear viscoelastic response.

Furthermore, it should be pointed out that in presented results failure strain increases with strain rate and also the maximum stresses rises with strain rates but at some point stress-strain curves become almost invariant to rate. This phenomenon is presented in Fig. 1a, which shows an influence of strain rate on the yielding process of the steel material and in Fig. 1b illustrating the comparison stress-strain characteristics of rubber-like materials in different strain rates.

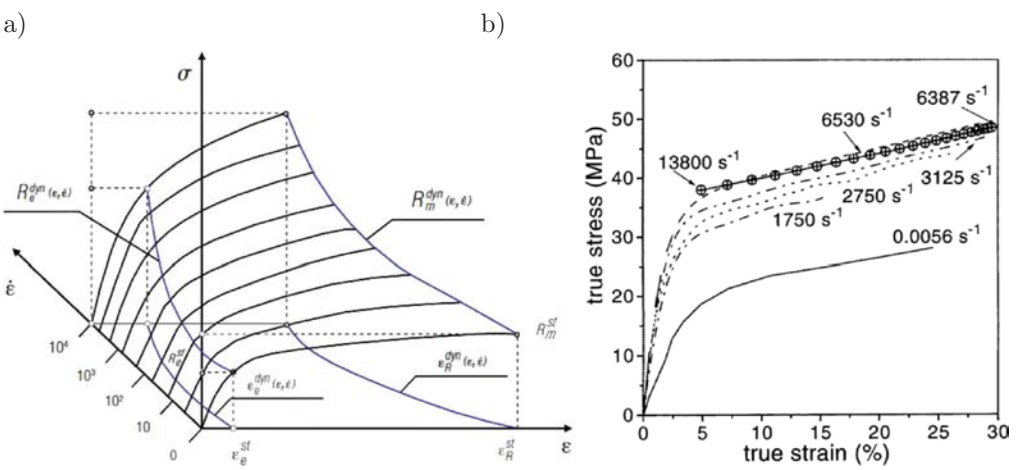

FIG. 1. a) Influence of strain rate on the yielding process of steel material [14] and b) comparison of stress/strain curves for rubber-like materials [3].

The authors of this paper decided to carry out numerical computations of an explosion under the terrain vehicle tire with suspension system. The main objective was to examine a dynamic behaviour of the tire with blast pressure propagation velocity taking into account, which together with other factors like strain rates, gas products characteristics, high reaction rate and exothermic effects have the biggest influence on how the detonation proceeds and what destruction it has [15, 16].

2. Analyses conditions

An object of investigations of presented researches is the suspension system with the tire. The major suspension system parts are: motor-car body, longitudinal, spring, axle, axle bush, hub, drum brake, steel rim and wheel. Geometries of the wheel and other suspension elements were achieved thanks to the reverse engineering technology [17, 18] (Fig. 2).

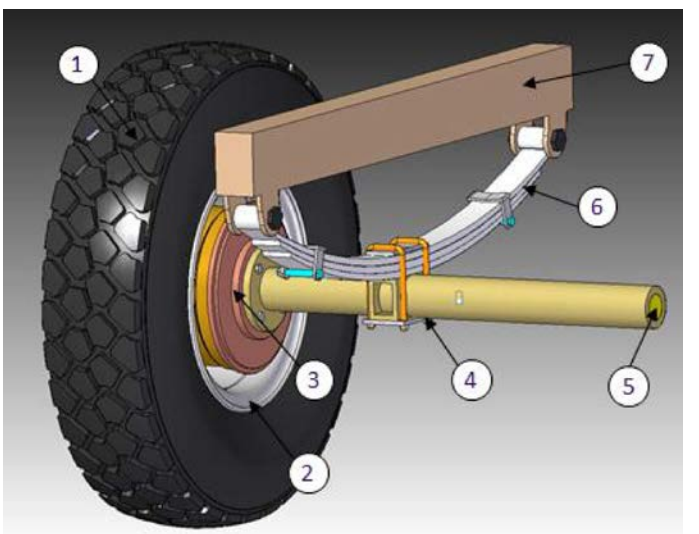

Fig. 2. Suspension system model, 1) Tire, 2) Drum brake, 3) Rim, 4) Axle bush, 5) Axle, 6) Spring, 7) Longitudinal and other hidden elements.

As mentioned before, material model with rate dependency (Ogden rubber-like material) and without rate effect taking into consideration (Mooney-Rivlin) were used in numerical analyses and results for both cases were compared. Material parameters for Mooney-Rivlin were estimated from one of the curves (for a quasi-static loading), which were used in Ogden rubberlike material also. Thus, in order to consider rate dependency in Ogden rubberlike material the load curve defining stress-strain characteristic of the material was replaced by the table with

a number of load curves defining the material response at the different strain rate (Fig. 3) [7]. Each material was implemented into the tire rubber major elements like tread and sidewall.

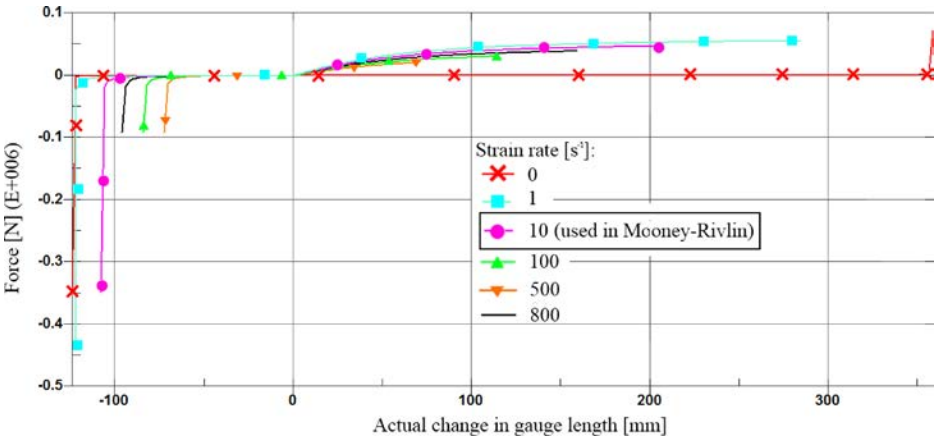

FIG. 3. Force *versus* actual change in gauge length for different strain rates [7].

Also, similar to the actual tire, steel cords were arranged inside radially and circumferentially [20–22]. A detailed description of the tire modelling can be found in the previous authors literature [17, 18]. FE model of the tire (without tread) is presented in Fig. 4.

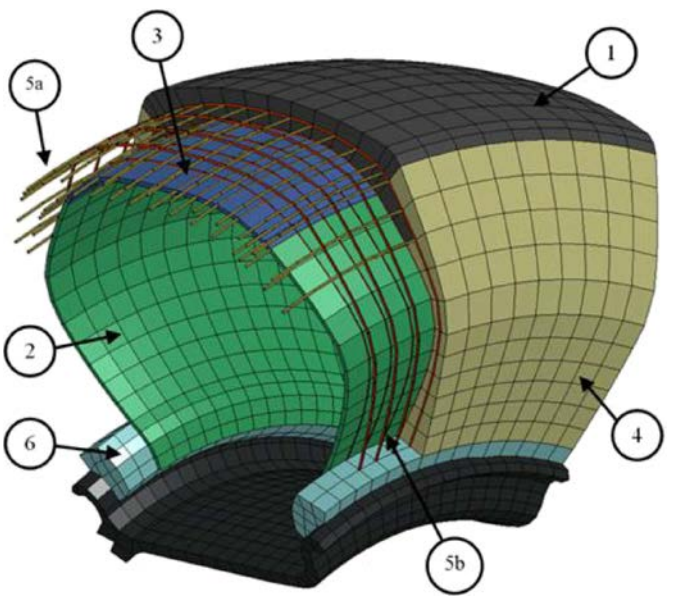

FIG. 4. FE tire model components (1. Tread, 2. Inner fabric, 3. Carcass, 4. Sidewall, 5a. Circumferential cords, 5b. Radial cords, 6. Bead core with cords) [17, 18].

In presented researches previously developed suspension system with the tire was subjected to a dynamic loading, more precisely, to pressure wave generated from the TNT explosion. Dynamic simulations were performed using the explicit LS-Dyna code using Arbitrary Lagrangian-Eulerian formulation with Jones Wilkins Lee (JWL) equation defining the explosive material [23]. Suspension system presented in Fig. 2 was modified by adding a simplified motor-car body, which simulated reflection effects of the pressure wave [17, 18]. All steel-like components were modeled using steel material with parameters taken from literature [19]. Due to the symmetric geometry of the vehicle (suspension system) only one wheel was taken into account (Fig. 5).

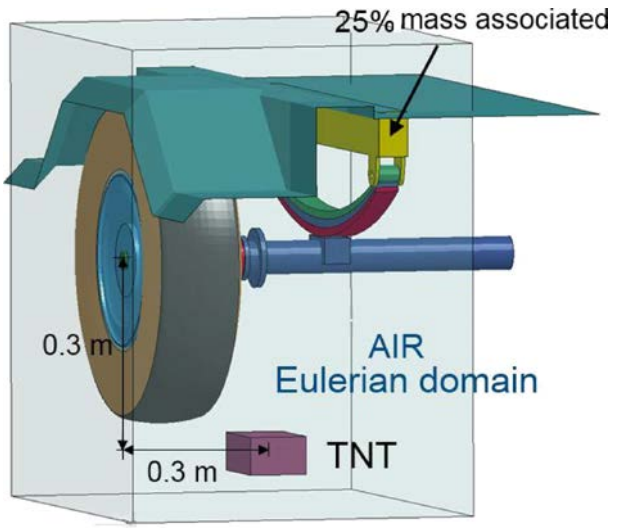

Fig. 5. Suspension system with ALE blast modeling.

Tire pressure was simulated using airbag model with Green function closed volume integration [23].Tire destruction effect caused by the explosion was simulated using the failure criterion based on the effective strain failure variable. As stated before, in simulations authors used TNT charge with the total mass of 6.34 kg according to NATO STANAG 4569 standard. Charges were located 0.3 m under the wheel and displaced by 0.3 m towards the end of axle. Consequently, results from both analyses were compared with two described earlier constitutive tire rubber models taking into consideration.

3. Explosion process description

In presented investigations for explosion simulation the Arbitrary Lagrangian-Eulerian formulation was used, where it was necessary to define an Eulerian air

domain, in which the explosive pressure wave propagates. Additionally, on the outer walls of it a non-reflecting option was applied, which considers the flow of the pressure outside the domain. The air is considered as simple ideal gas with linear polynomial equation of state [23]:

$$p = (C_4 + C_5\mu)\, E, \tag{3.1}$$

where $\mu = \rho/\rho_0$: ρ is density, ρ_0 is initial density; C_4 and C_5 are polynomial equation coefficients, E is internal energy.

The ALE procedure consists of two major steps: the classical Lagrangian step and the advection Eulerian step. The advection step is carried out with the assumption that nodes displacements are very small in comparison to characteristics of elements surrounding these nodes, e.g. dimensions. Moreover, in this procedure a constant topology of mesh is provided.

The governing equations for the fluid domain (Euler domain) describe the conservation of mass, momentum and energy [23]:

$$\frac{dM}{dt} = \frac{d}{dt}\int\limits_{V(t)} \rho\, dV = \oint\limits_{S(t)} \rho(\underset{\sim}{w} - \underset{\sim}{v}) \cdot \underset{\sim}{n}\, dS, \tag{3.2}$$

$$\frac{d\underset{\sim}{Q}}{dt} = \frac{d}{dt}\int\limits_{V(t)} \rho\underset{\sim}{v}\, dV = \oint\limits_{S(t)} \rho\underset{\sim}{v}(\underset{\sim}{w} - \underset{\sim}{v}) \cdot \underset{\sim}{n}\, dS - \int\limits_{V(t)} \nabla p\, dV + \int\limits_{V(t)} \upsilon\underset{\sim}{g}\, dV, \tag{3.3}$$

$$\frac{dE}{dt} = \frac{d}{dt}\int\limits_{V(t)} \rho e\, dV = \oint\limits_{S(t)} \rho e(\underset{\sim}{w} - \underset{\sim}{v}) \cdot \underset{\sim}{n}\, dS - \int\limits_{S(t)} p\underset{\sim}{v} \cdot \underset{\sim}{n}\, dS + \int\limits_{V(t)} \rho\underset{\sim}{g} \cdot \underset{\sim}{v}\, dV, \tag{3.4}$$

where ρ is fluid mass density; p is pressure; $\underset{\sim}{g}$ is acceleration of gravity; e is total specific energy. The quantities M, Q and E are total mass, total momentum and total energy, respectively, of a control volume $V(t)$, bounded by a surface S, which moves in the fluid (gas-air) with arbitrary velocity $\underset{\sim}{w}$ which may be zero in Eulearian coordinates or $\underset{\sim}{v}$ in Lagrangian coordinates. The vector $\underset{\sim}{n}$ is the outwards normal to the surface S.

In both cases it was necessary to implement the detonation process of the high explosive material into the model using so called "explosive burn" material model. In this approach the energy of high explosive (HE) material is assumed to be suddenly released inside the front of detonation wave. Detonation process requires to model the movement of the products of detonation (PD) after they reach subsequent specific locations by the detonation wave (DW) front. Applied

explosive burn model was modelled with the JonesWilkinsLee (JWL) equation of state with the following form [23]:

$$p = A\left(1 - \frac{\omega}{R_1\overline{\rho}}\right)\exp(-R_1\overline{\rho}) + B\left(1 - \frac{\omega}{R_2\overline{\rho}}\right)\exp(-R_2\overline{\rho}) + \frac{\omega\overline{e}}{\overline{\rho}}\frac{dE}{dt} = \frac{d}{dt}, \tag{3.5}$$

where $\rho = \rho_{he}/\rho$ is density of products of detonation; $e = \rho_{he}e$ is specific internal energy of PD; ρ_{he} refers to density of HE; p represents pressure of PD; A, B, R_1, R_2, ω are empirical constants determined for the specific type of HE

Table 1. TNT parameters for the JWL equation of state [19, 24].

Material	ρ [kg/m^3]	A [Pa]	B [Pa]	R1 [–]	R2 [–]	ω [–]
TNT	1630	3.712e+11	3.231e+9	4.150	0.900	0.3

4. Rubber constitutive models

Two chosen constitutive materials laws which are available in LS-Dyna package were investigated: Mooney-Rivlin material model, which doesn't include strain rates and Ogden rubberlike with rate-dependency option. Both are within a large group of materials which behave differently during loading (Fig. 6) and their constitutive relationship between stress and strain is formulated by nonlinear elasticity theory, called hyperelasticity [25–27].

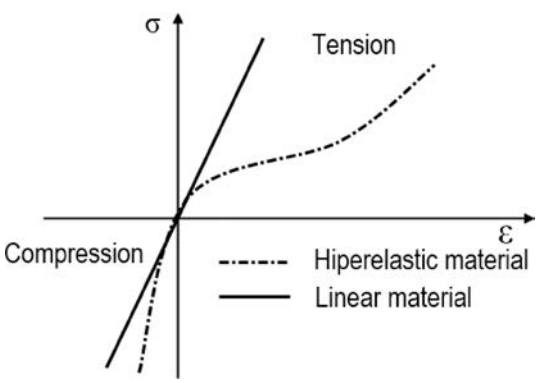

Fig. 6. Stress-strain curve for (non-linear) hyperelastic material [25].

A hyperelastic material is path independent and allows calculating the second Piola-Kirchhoff stress tensor [23, 26, 27]:

$$\mathbf{S} = 2\frac{\partial W}{\partial \mathbf{C}}, \tag{4.1}$$

where $W = \widehat{W}(\mathbf{C})$ – is a derivative of the energy functional, $\mathbf{C} = \mathbf{F}^T\mathbf{F}$ – is a right Cauchy-Green strain tensor ($\mathbf{F} = \mathrm{Grad}\,\mathbf{x}$).

In LS-Dyna two families of hyperelastic materials can be found. The first one is based on energy functional expressed in the invariants of the right Cauchy-Green tensor [23, 26, 27]:

$$W = \widehat{W}\left(I_1, I_2, I_3\right), \tag{4.2}$$

where

$$I_1 = \mathbf{1} : \mathbf{C} = tr\,\mathbf{C}, \qquad I_2 = \frac{1}{2}\left(I_1^2 - \mathbf{C} : \mathbf{C}\right), \qquad I_3 = \det \mathbf{C}.$$

Then, the derivative yields is given by [23, 26, 27]:

$$\mathbf{S} = 2\frac{\partial W}{\partial I_1}\mathbf{1} + 2\frac{\partial W}{\partial I_2}\left(I_1\mathbf{1} - \mathbf{C}\right) + 2\frac{\partial W}{\partial I_3}I_3\mathbf{C}^{-1}. \tag{4.3}$$

The Cauchy stress $\boldsymbol{\sigma}$ can now be obtained by $\boldsymbol{\sigma} = J^{-1}\mathbf{F}\mathbf{S}\mathbf{F}^T$, where $J = \det \mathbf{F}$ is the relative volume.

The second family of hyperelastic materials is formulated in terms of principle stretch ratios. Thus, all expression should be rewritten in terms of principal stretches λ_i. After decomposition $\mathbf{F} = \mathbf{R}\mathbf{U}$, $\mathbf{R}$ is an orthogonal matrix $\mathbf{R}^T\mathbf{R} = \mathbf{I}$, $\mathbf{U}$ is a positive definite symmetric matrix $\mathbf{U}^2 = \mathbf{C} \equiv \mathbf{F}^T\mathbf{F}$, the invariants are given by:

$$\begin{gathered} I_1 = \lambda_1^2 + \lambda_2^2 + \lambda_3^2, \qquad I_2 = \lambda_1^2\lambda_2^2 + \lambda_2^2\lambda_3^2 + \lambda_1^2\lambda_3^2, \\ I_3 = \lambda_1^2\lambda_2^2\lambda_3^2 = J^2 \end{gathered} \tag{4.4}$$

and the Cauchy stress $\boldsymbol{\sigma}$ and the principal engineering stress τ can be obtained from [23, 26, 27]:

$$\sigma_i = \frac{1}{\lambda_j\lambda_k}\frac{\partial W}{\partial \lambda_i} \Rightarrow \lambda_j\lambda_k\sigma_i = \tau_i = \frac{\partial W}{\partial \lambda_i}. \tag{4.5}$$

One of the most popular rubber constitutive model which is also used in presented investigations is the Mooney-Rivlin model [19, 20, 25–27]. Mathematical description of this model includes the elementary function of strain energy W, which is an elementary strain tensor function:

$$W = A(I_1 - 3) + B(I_2 - 3) + C\left(\frac{1}{I_3^2} - 1\right) + D(I_3 - 1)^2, \tag{4.6}$$

where A (C_{10}) and B (C_{01}) are material parameters. The last two expressions with the parameters C and D are hydrostatic terms given by [23, 26, 27]:

$$C = 0.5A + B, \tag{4.7}$$

$$D = \frac{A(5\nu - 2) + B(11\nu - 5)}{2(1 - 2\nu)}, \tag{4.8}$$

where ν is Poisson's ratio.

The second material model used in computations is MAT Simplified Rubber, which is based on the Ogden law [7, 9, 23, 28, 29]:

$$W = \sum_{i=1}^{3}\sum_{j=1}^{n} \frac{\mu_j}{\alpha_j}\left(\lambda_i^{*\alpha_j} - 1\right) + K(J - 1 - \ln J) \tag{4.9}$$

$$\Rightarrow \quad \sigma_i = \sum_{p=1}^{n} \frac{\mu_p}{J}\left[\lambda_i^{*\alpha_p} \sum_{k=1}^{3} \frac{\lambda_k^{*\alpha_p}}{3}\right] + K\frac{J-1}{J},$$

where α_j are non-integer, $J = \lambda_1\lambda_2\lambda_3$ and $\lambda_i^* = \lambda_i J^{-1/3}$, K is a material parameter that controls the size enclosed by the failure surface.

In this material Ogden functional is internally determined from the uniaxial engineering stress-strain curve by defining a tabulated of the principal stretch ratio as follows [7, 9, 23, 28, 29]:

$$f(\lambda) = \sum_{p=1}^{n} \mu_p \lambda^{*\alpha_p} \Rightarrow \sigma_i = \frac{1}{J}\left[f(\lambda_i) - \frac{1}{3}\sum_{j=1}^{3} f(\lambda_j)\right] + K\frac{J-1}{J}. \tag{4.10}$$

5. Simulations results

From the performed analyses the tire destruction and overall suspension system elements deformation were obtained. The main aforementioned objective was to compare each material behaviour during TNT explosion. Firstly, the internal energy of the tire was compared, which characteristic is presented in Fig. 7. The comparison graph of stress *versus* strain for the selected finite element (closest to the explosive charge) is presented in Fig. 8. Strain rates characteristics for both type of explosives and both materials for the same finite element of the tire are shown in Fig. 9.

It can be noticed, that for the same moment of time the tire destruction isn't identical for both material models. As expected the most devastated element of the examined suspension system is the tire, which consumes most of the explosive energy. In the Ogden rubberlike material case generated pressure wave

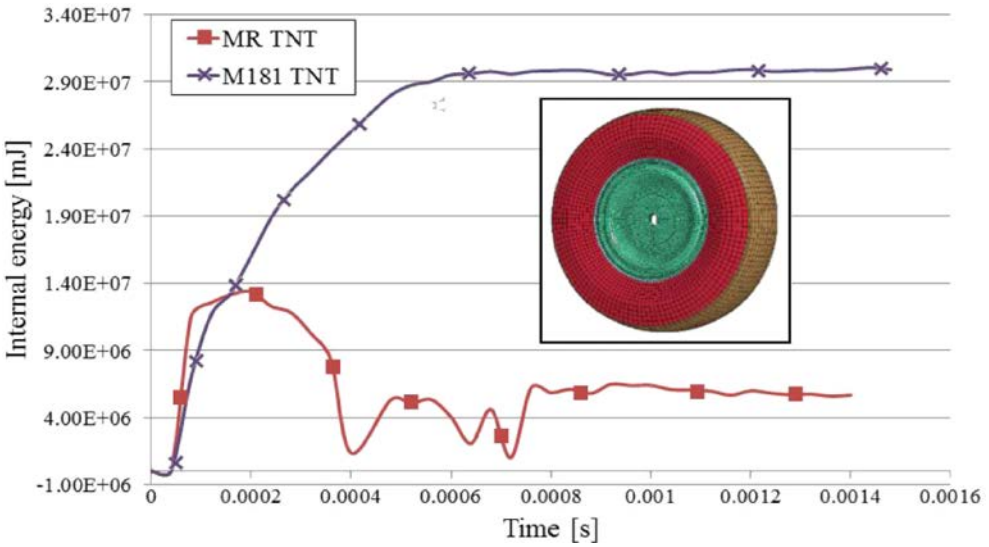

FIG. 7. Tire internal energy graph for all simulated cases.

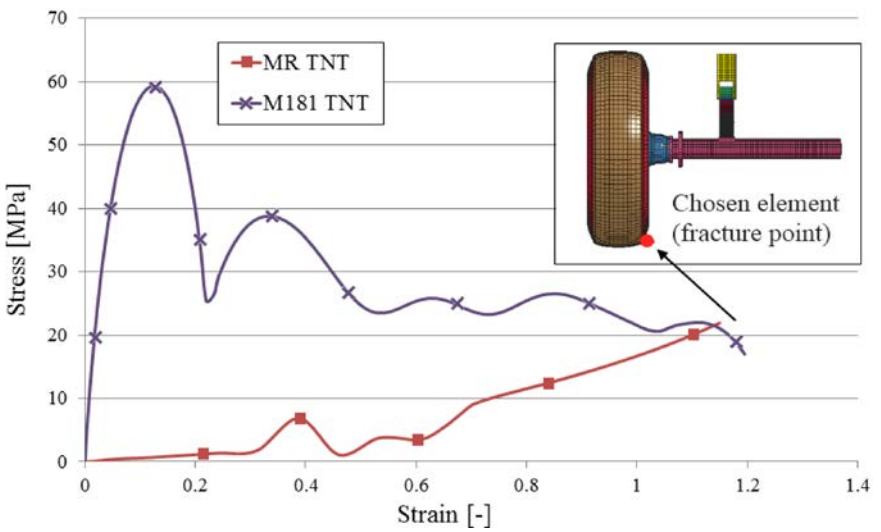

FIG. 8. Stress (equivalent) *versus* strain characteristics for all simulated cases (for selected tire element).

caused more damage to vehicle chassis elements, which means that more internal energy is absorbed by the tire what is clearly noticeable in Fig. 7. Obtained maximum energy values for Ogden rubberlike are approximately twice time bigger than for the Mooney-Rivlin material. Taking closer look at the stress (equivalent)-strain curves presented in Fig. 8 it can be also seen that maximum stress values for Ogden rubberlike are higher than for Mooney-Rivlin material

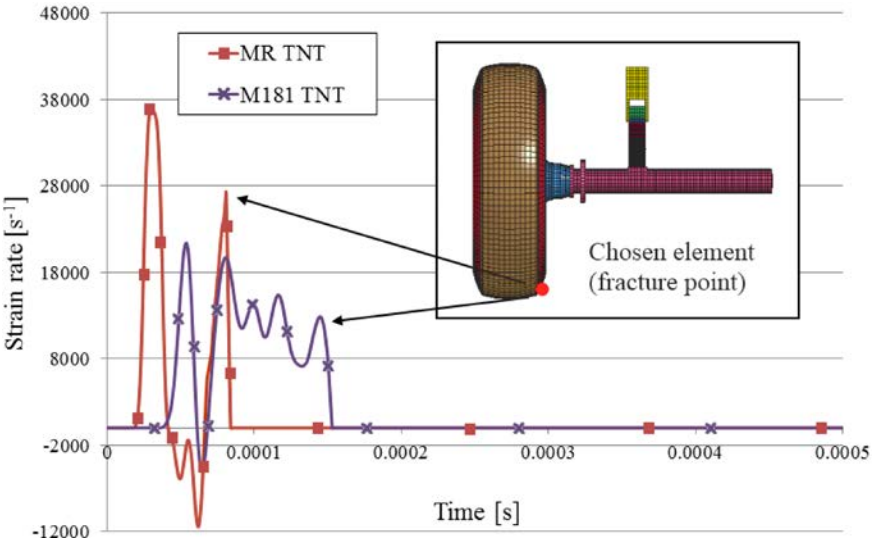

FIG. 9. Strain rate comparison for all cases (for selected tire element).

(about three times), which ideally reflects the strengthening effect presented in Fig. 1a, which indicates the strain-rate dependency not only on the element structure but also on its stresses. From the theoretical point of view it is known that the amount of absorbed energy directly depends on the stress value [23], which is very well presented in the following results for the chosen finite element. For Ogden rubberlike material equivalent stresses are higher (Fig. 8).

As mentioned before, for simulating the tire destruction effect the strain erosion criterion was applied with failure strain value of 120%. This value was obtained for both materials, however in Mooney-Rivlin material chosen element was deleted at approximately 117% strain value.

From Fig. 9 it can be seen that strain rates are different for both simulated materials. In Mooney-Rivlin case obtained maximum strain rates value was approximately 3.8e+4 s^1, whereas for Ogden rubberlike it was about 2.0e+4 s^1, which seems to be reliable if we take into account the results presented by other authors [3, 10–13]. This difference between rates for two materials indicates the absence of rate dependency in Mooney-Rivlin material.

6. Conclusions

The authors of the presented paper made an attempt of simulating a rubber structure, which in this case was the vehicle tire, under a dynamic blast wave loading. Performed analyses have completely confirmed destructive effect of the explosion under the vehicle chassis. As expected, the most devastated element

of the examined suspension system is the tire, which consumes the most of the detonation energy which results in its destruction. By implementing them into the discrete model of the investigated object a high accuracy of numerical solution is provided

Presented results shows, that by choosing the proper constitutive material for the specific phenomenon a high accuracy and reliability of numerical solution is provided. From the above results the general conclusion is that for such strongly dynamic phenomenon as blast explosion the material with rate dependency is necessity. In presented tests the authors used the strain-rate material characteristics taken from literature. Therefore, in subsequent stages the Ogden rubberlike material used in investigations will be more thoroughly tested with the particular attention pointed on its possible adoption into the vehicle tire model. Moreover, complex experimental tests of the rubber and rubber-cord composite within various loading velocities are planned, which will determine the strain rate effect on the material structure behaviour with failure process taking into account. Obtained rate dependency data will be then eventually used in final stages of carried out investigations.

Acknowledgment

The material presented in this paper has been shown at Workshop 2012 on Dynamic Behavior of Materials and Safety of Structures, Poznan, 2–4 May, 2012.

References

1. Ochelski S., Bogusz P., Kiczko A., *Influence of hardness on mechanical properties of elastomers*, Journal of KONES Powertrain and Transport, **17**, 317–325, 2010.
2. Krawczyk A., *Mechanics of polymer and composite materials*, Science, 1985.
3. Roland C.M., *Mechanical behaviour of rubber at high strain rates*, Rubber Chemistry and Technology, **79**, 429–459, 2006.
4. Chen W., Lu F., Frew D.J., Forrestal M.J., *Dynamic compressive testing of soft materials*, Journal of Applied Mechanics, **69**, 214–223, 2002.
5. Quintavalla S.J., Johnson S.H., *Extension of the Bergstrom-Boyce model to high strain rates*, Rubber Chemistry and Technology, **77**, 5, 972–981, 2005.
6. Song B., Chen W., *One-dimensional dynamic compressive behaviour of EPDM rubber*, Journal of Engineering Materials and Technology, **125**, 294–301, 2003.
7. LS-Dyna Aerospace Working Group, *Rubber Projectile Impacting a Rigid Plate*, 2012.
8. Chen Y., Zhang Z., Wang Y., Hua H., *Crush dynamics of square honeycomb thin rubber wall,* Thin-Walled Structures, **47**, 1447–1456, 2009.

9. Du Bois P.A., Kolling S., Fassnacht S., *Material behaviour of polymers under impact loading*, International Journal of Impact Engineering, **32**, 725–740, 2006.

10. Hoo Fat M.S., Bekar I., *High-speed testing and material modelling of unfilled styrene butadiene vulcanizates at impact rates*, Journal of Materials Science, **39**, 23, 6885–6899, 2004.

11. Bekar I., Hoo Fatt M.S., Padovan J., *Deformation and fracture of rubber under tensile impact loading*, Tire Science Technology, **30**, 45, 2002.

12. Al-Maliky N.S., Parry D.J., *A freely expanding ring technique for measuring the tensile properties of polymers*, Materials Science Technology, **7**, 746–752, 1996.

13. Gourdin W.H., Weinland S.L., Boling R.M., *Development of the electromagnetically launched expanding ring as a high-strain-rate test technique*, Review of Scientific Instruments, **60**, 427–432, 1989.

14. Kruszka L., *The study of static and dynamic properties of steel for safety and protective structures* [in Polish: *Badania eksperymentalne własności statycznych i dynamicznych stali budowlanych dla potrzeb konstrukcji ochronnych i obronnych*], Seminar Materials of Military University of Technology, 2008.

15. Morka A., Kwaśniewski L., Wekezer J., *Assessment of Passenger Security in Paratransit Buses*, Journal of Public Transportation, **8**, 47–63, 2005.

16. Lacome J.L., *Analysis of Mine Detonation, SPH analysis of structural response to anti-vehicles mine detonation*, LSTC, 2007.

17. Baranowski P., Małachowski J., *Blast wave and suspension system interaction- numerical approach*, Journal of KONES Powertrain and Transport, **18**, 2, 17–24. 2011.

18. Baranowski P., Małachowski J., Niezgoda T., *Numerical Analysis of Vehicle Suspension System Response Subjected to Blast Wave*, Applied Mechanics and Materials, **82**, 728–733, 2011.

19. Malachowski J., *Modelling and research of interaction between gas and pipe structures subjected to pressure impulse* [in Polish: *Modelowanie i badania interakcji ciało stałe-gaz przy oddziaływaniu impulsu ciśnienia na elementy konstrukcji rurociągu*], BEL Studio, Warsaw, 2010.

20. Neves R.R.V., Micheli G.B., Alves M., *An experimental and numerical investigation on tyre impact*, International Journal of Impact Engineering, **10**, 685–693, 2010.

21. Cho I.R., Kim K.W., Jeong H.S., *Numerical investigation of tire standing wave using 3-D patterned tire model*, Journal of Sound and Vibration, **305**, 795–807, 2007.

22. Helnwein P., Liu C.H., Meschke G., Mang H.A., *A new 3-D finite element model for cord-reinforced rubber composites- application to analysis of automobile tyres*, Finite Elements in Analysis and Design, **4**, 1–16, 1993.

23. Hallquist J.O., *LS-Dyna: Theoretical manual*, California Livermore Software Technology Corporation, 2003.

24. Włodarczyk E., *Introduction to the mechanics of explosion* [in Polish: *Wstęp do mechaniki wybuchu*], PWN, Warsaw, 1994.

25. ANSYS, *Hyperelasticity*, Structural Nonlinearities, 6, Second Edition Release 5.5, 1999.

26. Mooney M., *A theorie of elastic deformations*, Journal of Application Physics, **11**, 582–592, 1940.

27. Rivlin R.S., *Large elastic deformations of isotropic materials*, Philosophical Transactions of The Royal Society A, **240**, 459–490, 1948.

28. Benson D.J., Kolling S., Du Bois P.A., *A simplified approach for strain-rate dependent hyperelastic materials with damage*, 9th International LS-DYNA Users Conference, **15**, 29–36, 2006.

29. Ogden R.W., *Elastic deformations of rubberlike solids*, Mechanics of Solids, The Rodney Hill 60th Anniversary Volume, Oxford, 1982.

Received June 5, 2012; revised version December 7, 2012.